Supporting Materials

for

Lithium-Titanium Oxide Powder Morphology Correlation with High-Rate Performance in Lithium-ion Batteries

Hermes A. Llaín-Jiménez [1], Dominika A. Buchberger [1], Magdalena Winkowska-Struzik [2,#,*], Maciej Ratyński [1], Michał Krajewski [1], Maciej Boczar [1], Bartosz Hamankiewicz [1,*], Andrzej Czerwiński [1,*]

[1] Faculty of Chemistry, University of Warsaw, ul. Ludwika Pasteura 1, 02-093 Warsaw, Poland
[2] Łukasiewicz-Institute of Microelectronics and Photonics, al. Lotników 32/46, 02-668 Warsaw, Poland
[#] Current address: Faculty of Chemistry, University of Warsaw, ul. Ludwika Pasteura 1, 02-093 Warsaw, Poland
* Correspondence: MW-S: m.winkowska@chem.uw.edu.pl; BH: bhamankiewicz@chm.uw.edu.pl; AC: aczerw@chem.uw.edu.pl

Tab. S1. High-rate performance and characteristics of several LTO materials found in literature.

Starting materials / synthesis details	Specific Surface Area, BET [$m^2 g^{-1}$]	Particle size / SEM, TEM	Crystallite size XRD [nm]	Electrode mass loading [$mg\ cm^{-2}$]	Capacity @1C [$mAh\ g^{-1}$]	Capacity @10C [$mAh\ g^{-1}$]	Ref.
Sol-gel							
$Ti(OC_4H_9)_4$ and CH_3COOLi /with citric acid as chelating agent	-	150-600 nm (SEM)	-	-	159	147.7	[37]
$Ti(OC_3H_7)_4$ and CH_3COOLi / Pluronic P123 as chelating agent in CH_3OH/HNO_3	-	100 nm (SEM)	-	2	180	150	[70]
$Ti(OC_4H_9)_4$ and LiOH	2	200-500 nm (SEM)	-	1.4-1.7	123.1 (@5C)	102.5	[48]
TiN and LiOH in H_2O / CH_3OH sol. with H_2O_2 and NH_4OH	2.2	200 nm (SEM)	-	2	159.5	20	[49]
TiO_2 (self-made) and LiOH in conc. HNO_3	2.48	c.a. 300 nm (SEM)	-	2.5	106	49.9	[50]
$Ti(OC_4H_9)_4$ and CH_3COOLi / citric acid as complexing agent	5.33	380 nm (SEM)	-	-	168.2	143	[41]
Combustion							
Citric-nitrate combustion synthesis / $Ti(OC_4H_9)_4$ and $LiNO_3$ in ammonia/ethanol mixture	-	500 (SEM)	-	1.5	157	115	[68]
$TiO(NO_3)_2$ (self-made) and $LiNO_3$ with cellulose fiber - combustion in Glycine-nitrate	3.07	-	33.1	-	160	125	[69]
$TiO(NO_3)_2$ (self-made) and $LiNO_3$ with glycine as a fuel - combustion in solution	12	-	80	4	160 (@0.5C)	140	[51]
Solid state reaction							
TiO_2 and LiOH	-	500 nm (SEM)	-	5.5	149	103.9	[52]
TiO_2 and Li_2CO_3 (Urea-assisted)	-	400 nm (SEM)	-	-	165	126.9	[42]
TiO_2 and Li_2CO_3 (Microwave-assisted)	-	180 nm (SEM)	-	-	163	111	[71]

TiO_2 and Li_2CO_3	-	424 nm (SEM)	-	5.5	152.7	104.6	[43]
TiO_2 and Li_2CO_3	4.4	200-500 nm (SEM)	87	2.76	168	105.7	[30]
TiO_2 and Li_2CO_3	18.3	162 nm (SEM)	-	-	171	139	[58]
Supercritical solvents							
$Ti(OC_3H_7)_4$ and LiOH / supercritical water	10	150-200 nm (SEM)	-	-	193	160	[61]
$Ti(OC_3H_7)_4$ and LiOH / supercritical methanol	57.8	-	11-62	-	173.9	108.5	[46]
Spray-drying							
$Ti(OC_3H_7)_4$ and CH_3COOLi / acetylacetone as chelating agent	12.04	500 nm (SEM)	-	-	144	100	[65]
Not specified							
Pilot-scale process (details not specified), end process: intensive grinding	22	50-250 nm (SEM)	-	4.6-4.7	159	135	[36]
Microemulsion synthesis							
$Ti(OC_3H_7)_4$ and LiOH / CTAB-assisted synthesis in n-pentanol and cyclohexane	46.3	30-50 nm (TEM)	-	-	166	130	[67]
Solvothermal							
Solvothermal synthesis / $Ti(OC_4H_9)_4$ and LiOH with glycine	54.8	100-500 nm (SEM)	-	1.3	154	146	[44]
Hydrothermal							
CH_3COOLi and $Ti(OC_4H_9)_4$ - (rheological phase reaction)	-	< 3 μm (SEM)	-	-	161.6	140.2	[72]
$TiOSO_4$ and LiOH	-	-	12.5	-	147.3 (@1.1C)	128 (@11.4C)	[73]
TiO_2 and LiOH (Microwave-assisted)	-	40 nm (SEM)	-	1.49	174	148	[66]
$Ti(OC_3H_7)_4$ and LiOH in ethylene glycol and NH_4OH	-	c.a. 200 nm (SEM)	-	-	163	152 (@8C)	[74]

$Ti(OC_3H_7)_4$ and CH_3COOLi	-	c.a. 300 nm (SEM)	-	-	132	105	[47]
$Ti(OC_3H_7)_4$ and LiOH (CTAB-assisted)	19.93	c.a. 300 nm (SEM)	-	3.5	162.3	144.9	[60]
$Ti(OC_3H_7)_4$ or $Ti(OC_4H_9)_4$ and LiOH / with H_2O_2 (Microwave-assisted)	20	-	40	4	150	120	[64]
TiO_2 and LiOH	36.76	40 nm (TEM)	-	20	172	165	[56]
$Ti(OC_4H_9)_4$ and LiOH in ethylene glycol / CTAB assisted	38.6	4 μm (SEM)	21	1.1	164	154	[54]
TiO_2 (self-made) and LiOH	40	10 nm plates (SEM)	-	-	144	133	[63]
$Ti(SO_4)_2$ and LiOH with glycerol	85.93	25 nm (TEM)	-	-	170	165	[57]
$TiOSO_4$ and LiOH	112.3	40-60 nm (TEM)	-	-	170	150	[45]
amorphous TiO_2 (self-made) and LiOH	131.2	c.a. 200 nm (SEM)	-	2	160	151	[55]
$Ti(OC_3H_7)_4$ and LiOH	139.4	-	12	-	177 (@1.1C)	161 (@14C)	[59]
$Ti(OC_4H_9)_4$ and LiOH in EtOH	150.6	c.a. 200 nm (SEM)	-	6.5	169	158	[53]
TiO_2 and LiOH, NaOH and H_2O_2-assisted (3-step)	178	6.6 nm sheets (TEM)	-	-	179	162	[62]

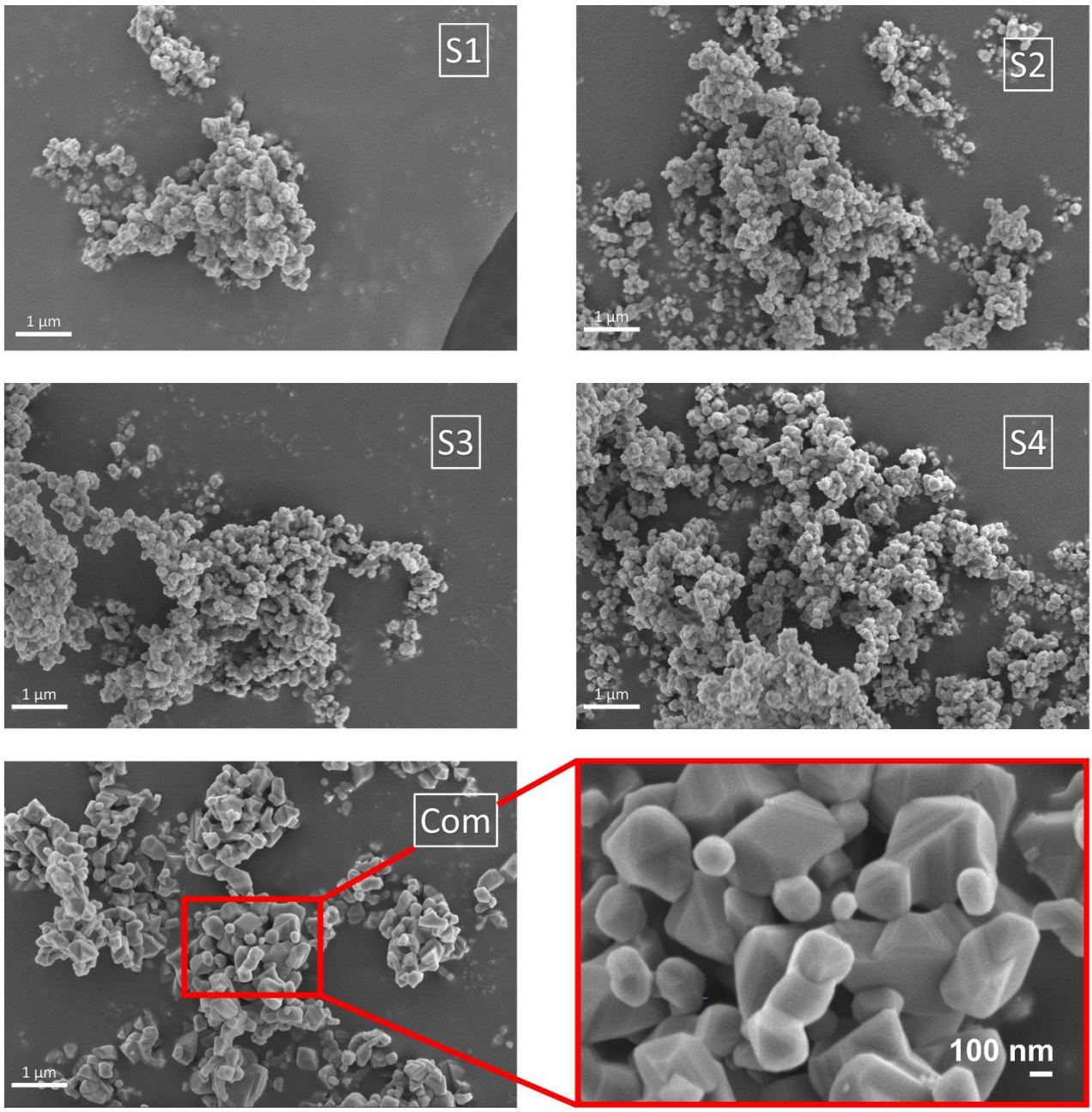

Fig. S1. SEM images for the sol-gel synthesized and commercial LTO samples with reference to 1µm.

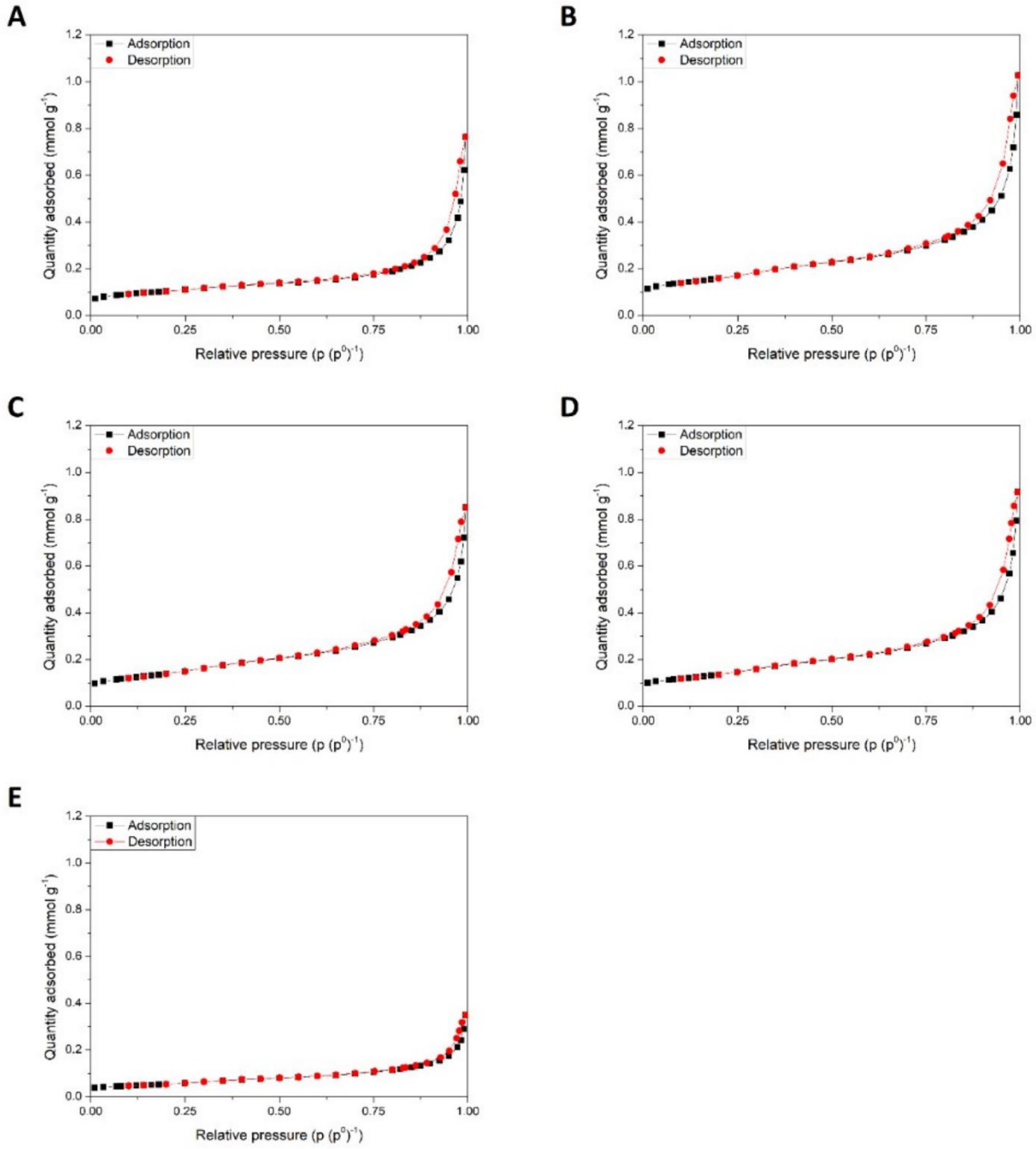

Fig. S2. N_2 adsorption/desorption isotherms of $Li_4Ti_5O_{12}$ powders: S1 (A), S2 (B), S3 (C), S4 (D) and Com (E).

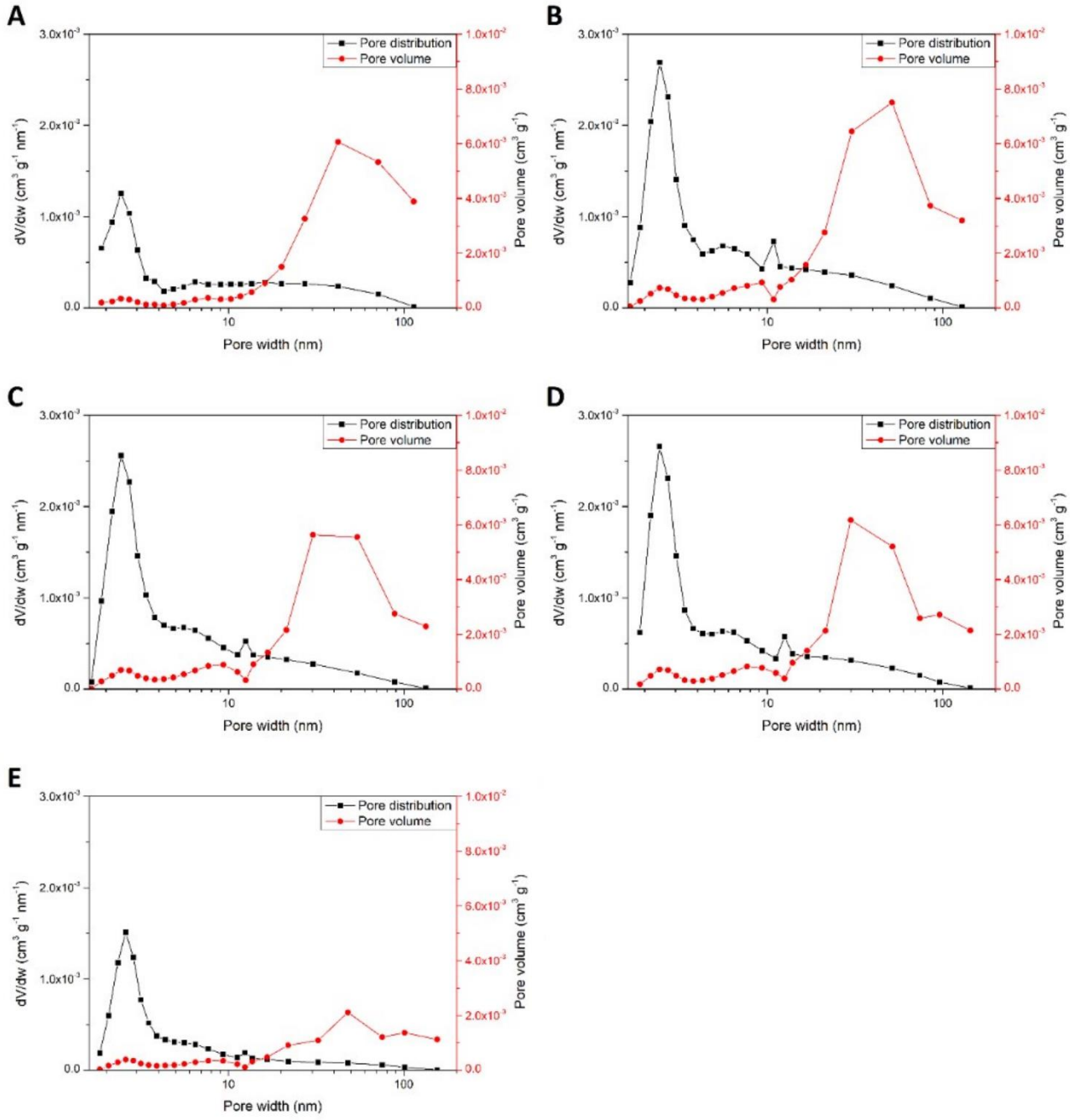

Fig. S3. Pore size and distribution for $Li_4Ti_5O_{12}$ powders: S1 (A), S2 (B), S3 (C), S4 (D) and Com (E).

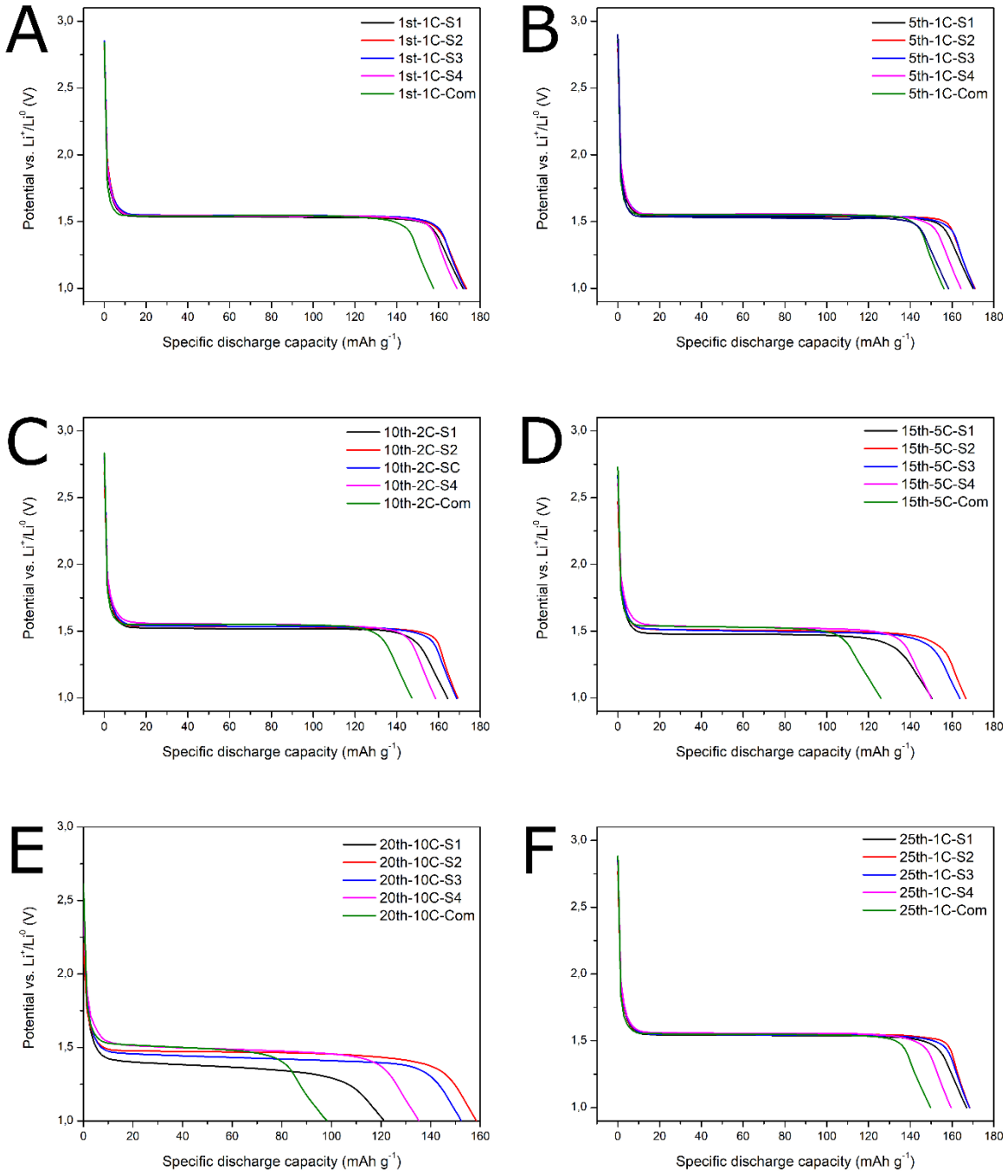

Fig. S4. Discharge curves of sol-gel obtained and commercial LTO samples. A) 1st cycle at 1C, B)5th cycle at 1C, C)10th cycle at 2C, D) 15th cycle at 5C, E) 20th cycle at 10C, F) 25th cycle at 1C

Figure S4 shows the behaviour of the different discharge curves for all samples at all rates. It is notable how the samples hold a similar behaviour at the initial 1C cycling. The most remarkable

difference is the bigger specific capacity value for the sol-gel synthesized samples respect to the commercial samples. The behaviour is kept as the discharge rate increases to 2C with a corresponding decrease in the discharge specific capacity. At 5C the lost in specific capacity for the commercial materials is around 18% and increases to approximately 40% at 10C. The plateau values for all samples decrease as the current increases as a consequence of the polarization of the cells. The bigger the polarization, the bigger the difference in the plateau at different currents and the bigger the internal resistance within the cell. It could be expected that the higher the plateau, the higher the capacity but this is not always the case. For example, sample S1 at 10C presents a higher discharge capacity than the commercial samples even though its plateau drop is bigger than for the commercial samples. The performance of the materials in term of specific energy of an operational cell will depend on both the discharge specific capacity and its plateau value: the highest the plateau and the bigger the specific capacity, the bigger the energy released by a cell.

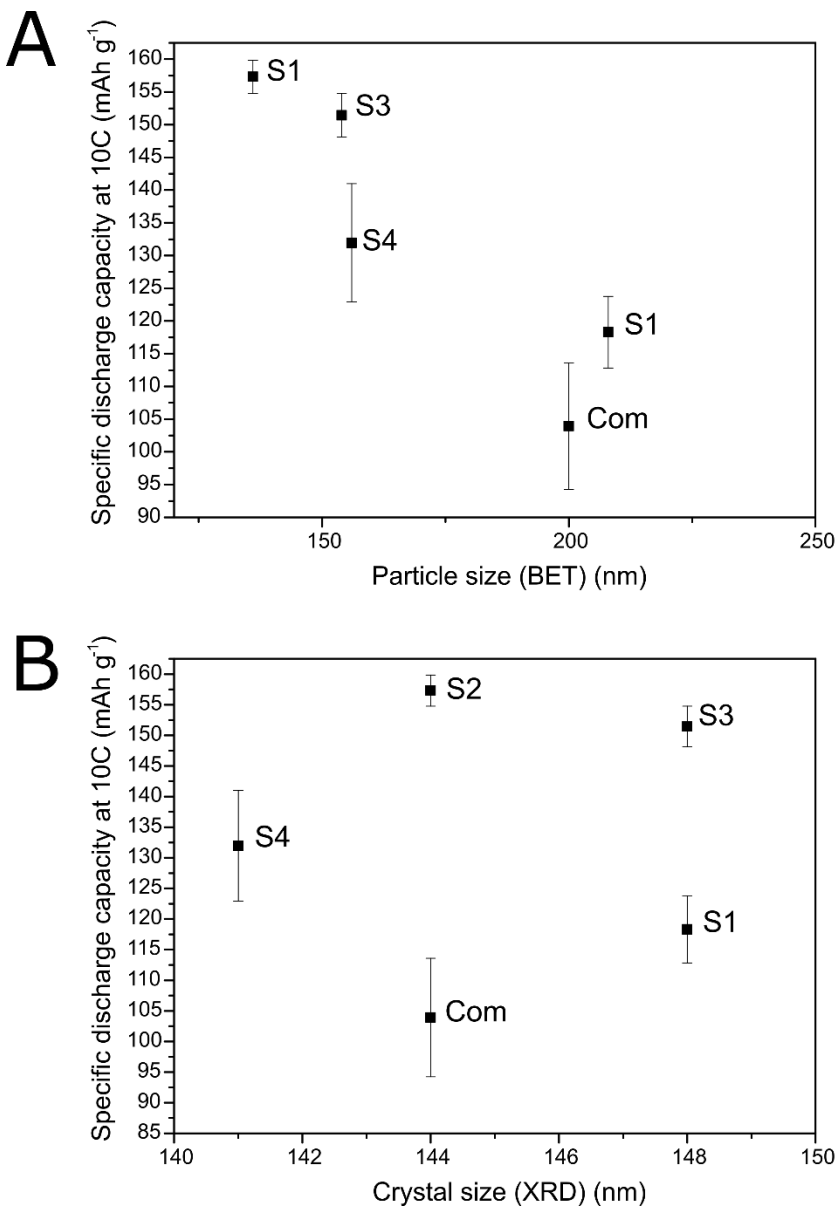

Fig. S5. The relation between specific discharge capacity at 10C (SDC10C) and (A) particle size calculated by BET and (B) crystal size calculated by XRD.

Figure S5 shows that the relation of the specific discharge capacity at 10C and particle size is similar to the one between SDC10C and specific surface area. At the end, both parameters are calculated from the same experimental results and alike models. It is important to keep in mind the limitations of the calculation of particle size by the BET method since many approximations are being used. For

example, that the particles are spheres. The non-existing relation between SDC10C and crystal size shows the independence of the high-rate performance of this structural characteristic.